

# Spatiotemporal variation analysis of slant wet delays from one GPS station over China

## Introduction

Almost all the current GNSS software only output products, like ZTD, ZWD, and gradients, with a given time resolution at the given GNSS station. In this case, obtaining a spatial map of atmosphere water vapor requires a dense network of GNSS stations. However, for many areas (such as mountains, small islands), there are not dense GNSS stations. Thus, it is difficult to analyze the spatial variations of water vapor in such areas. Zhang et al. (2020) proposed a method to model Slant Wet Delays (SWDs) derived from one GNSS station. This approach permits to study spatiotemporal variations of the water vapor field as seen from one GNSS receiver without dense GNSS stations. Thus, in this research, we apply the modeling method in 22 selected GPS stations over China to analyze the SWDs variations with elevation and azimuth.

## Data and methodology

### Data and processing

- ✓ Altogether 22 stations from the Crustal Movement Observation Network of China (CMONOC), as displayed in Fig. 1, covering the period from Jan, 1, 2018 to Dec, 31, 2018 were selected. GPS stations are grouped in different colors based on the climate types
- ✓ The details of the GPS data processing strategy are given in Tab. 1
- ✓ The integrity rates of the estimated ZTD products are displayed in Fig. 2

### Modelling SWDs

Our strategy to retrieve the SWDs is:

$$SWD = m_{f_{wet}}(\varepsilon) \cdot [ZWD + \cot(\varepsilon) (G_N \cdot \cos(\theta) + G_E \cdot \sin(\theta))]$$

$$ZWD = ZTD - ZHD \quad ZHD = 2.2768 P_s / f(\lambda, H)$$

For the pressure  $P_s$ , we used the data from ERA5 products

The method (Zhang et al., 2020) translated the modeled SWDs to an almost stationary process with the respect to the elevation by considering the quantity:  $SE = SWD * \sin(\varepsilon)$

Then, this method wrote SE as a function of time (t), elevation ( $\varepsilon$ ) and azimuth (a), as seen from the GPS receiver, as:

$$SE(t, \varepsilon, \alpha) = \sum_{n=0}^N \sum_{l,m=0}^L C_{n,l,m} P_n(t) Y_{l,m}(\varepsilon, \alpha)$$

where the  $P_n$  are orthonormal functions, and  $Y_{l,m}$  are spherical harmonics functions. By using a least-squares fit and fixing  $\varepsilon$  and  $\alpha$  to priori values, we can determine the coefficients  $C_{n,l,m}$ . In this way, we can reconstruct the SE signals over the hemisphere, as well as their time evolutions.

## Results

### ZTD error analysis

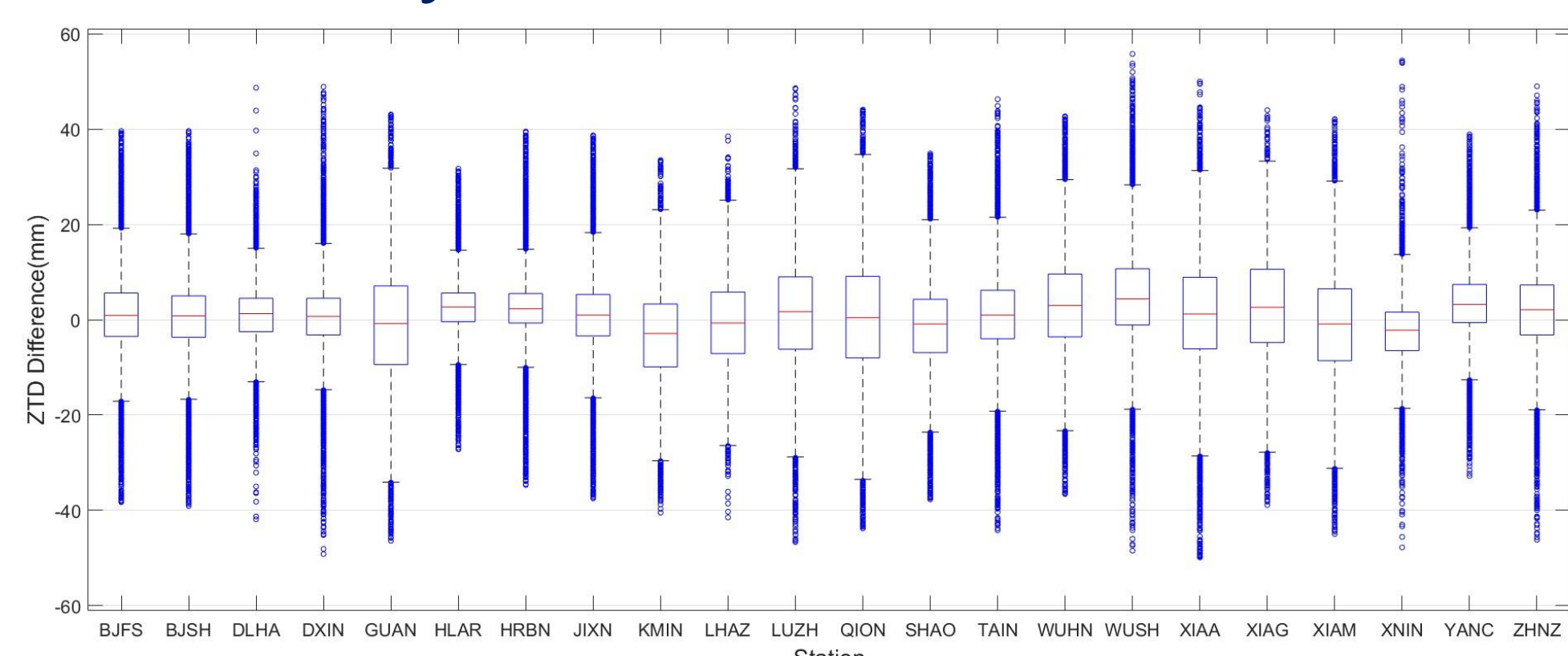


Fig.3 Boxplots of ZTD differences between ERA5 and GPS for all stations

#### Sub results

- ✓ The mean value of the differences between ERA5 ZTDs and estimated GPS ZTDs at all stations is 0.81 mm
- ✓ The mean STD and RMS of ZTD differences between GPS and ERA5 are 10.40 and 10.70 mm

### Validation of the modeling SWDs method

Tab. 2 Location of the collocated stations

Station	Latitude (°)	Longitude (°)	Height(m)	Distance(m)	Dh(m)
LHAZ	29.6573	91.1040	3624.6221	0.07	0.0031
LHAS	29.6573	91.1040	3624.6190		
SHAO	31.0996	121.2004	22.0451	0	0.0591
SHA2	31.0996	121.2004	21.9860		

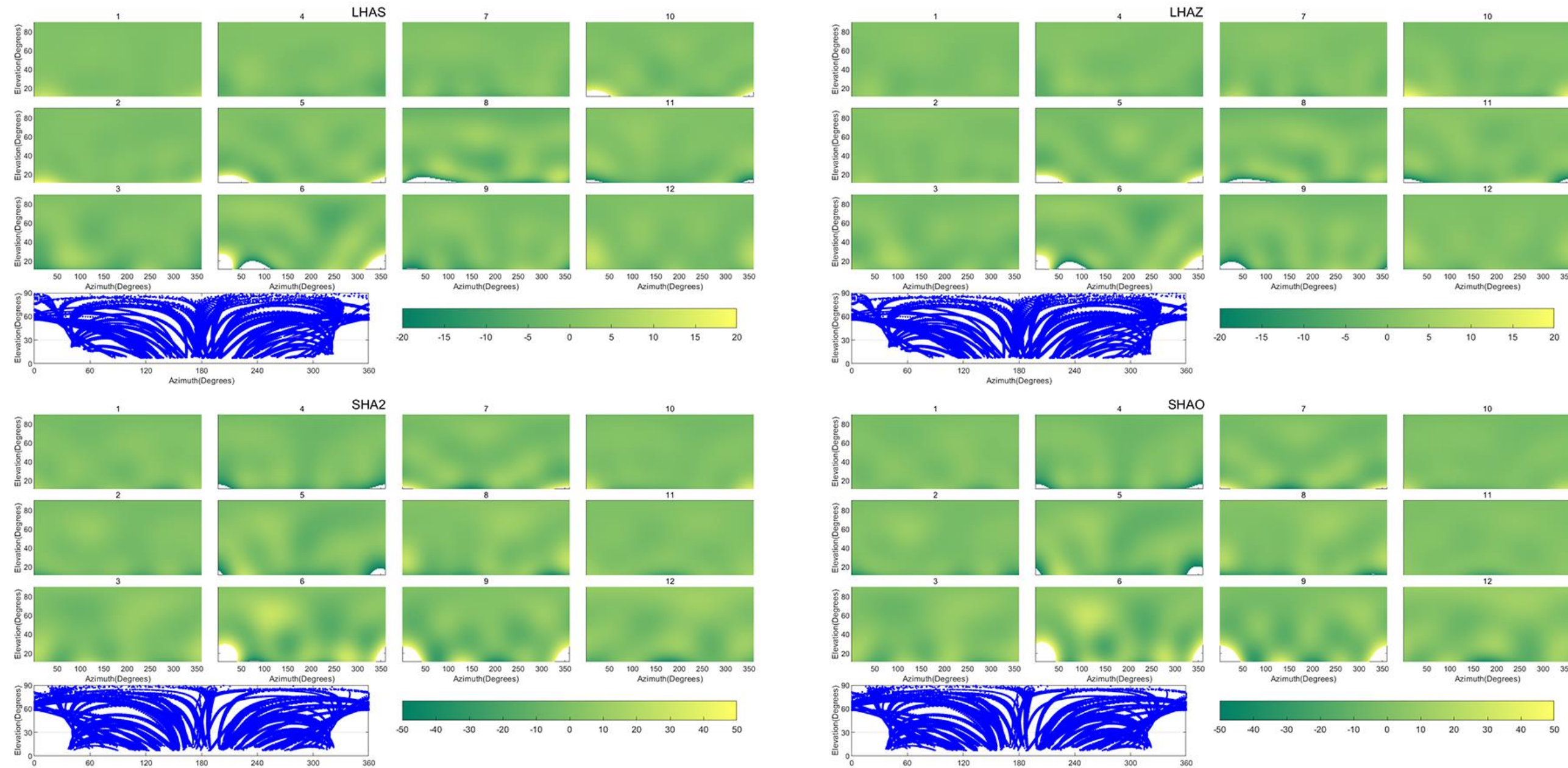


Fig.4 Sky view of SE signals at the middle of each month in 2018 and sky tracks of the GPS satellites visible from the GPS stations in 2018. (Colorbar: the variations of the SE values in mm)

#### Sub results

- ✓ The mean of ZTD differences between LHAS and LHAZ is -1.5 mm and the STD is 3.1 mm. For SHA2 and SHAO, the mean of ZTD differences is -1.7 mm and the STD is 3.0 mm
- ✓ The variations of SE values in space and time are almost completely same for each pair of collocated stations

Tab. 1 Data processing strategies for GPS observations

Simple interval	300s
Frequency combination	Ionosphere-free combination
Elevation cut-off angle	$\theta_c = 1^\circ; e > 30^\circ; p = 2 \sin(e), e \leq 30^\circ$
Elevation weighting strategy	
Phase center correction	igsR3_2135.atx
Mapping function	VMF3
Satellite orbits	Fixed to IGS repro3 products
Satellite clocks	Fixed to estimated 5 min products
Coordinates	Constant parameter
ZTD stochastic model	Piece-wise constant (1h), random walk between segments (15mm/ $\sqrt{h}$ )
Gradient mapping function	$m_{f_w} \cdot \cot(e)$ (Bar-Sever et al., 1998)
Gradient stochastic model	Piece-wise constant (1h), random walk between segments (10mm/ $\sqrt{h}$ )

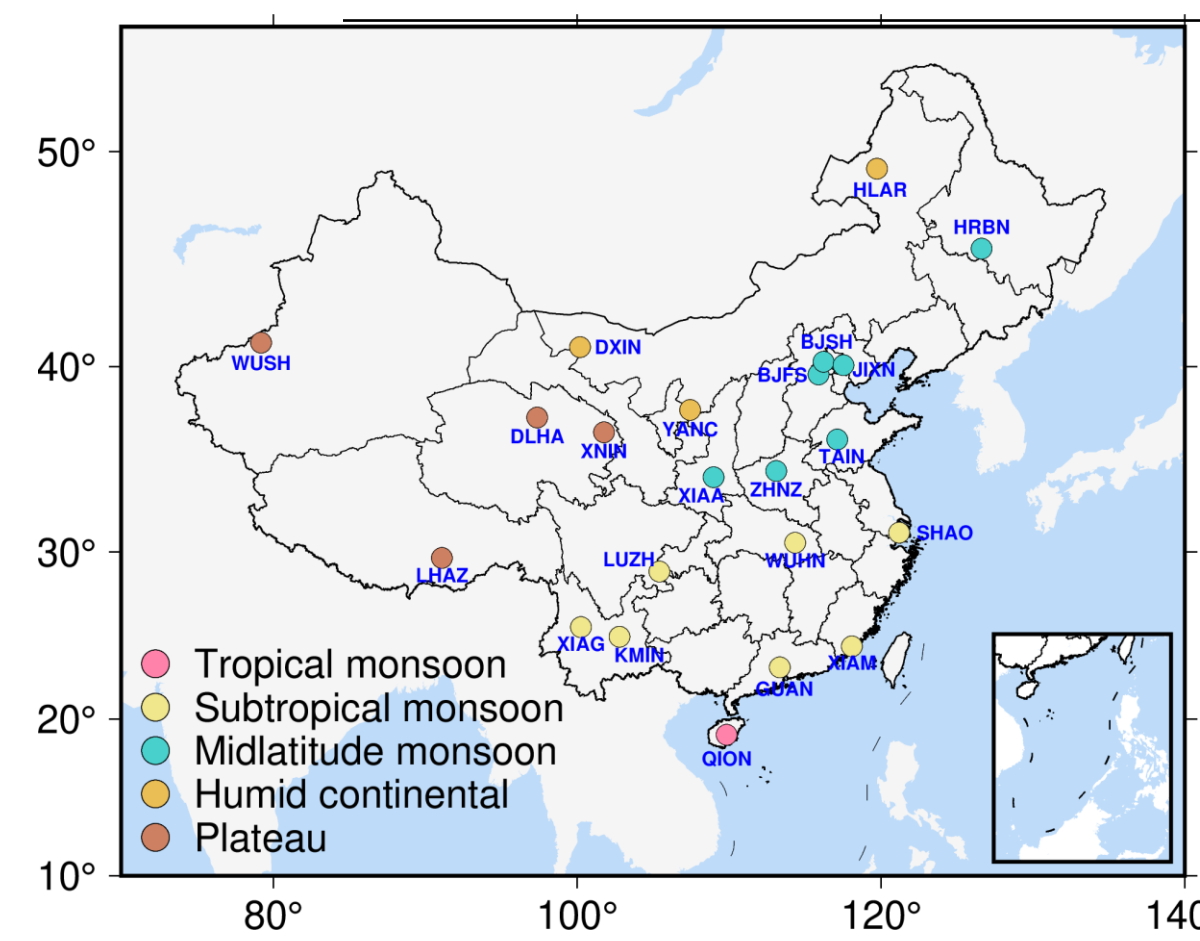


Fig.1 Geographical distribution of the selected GPS stations

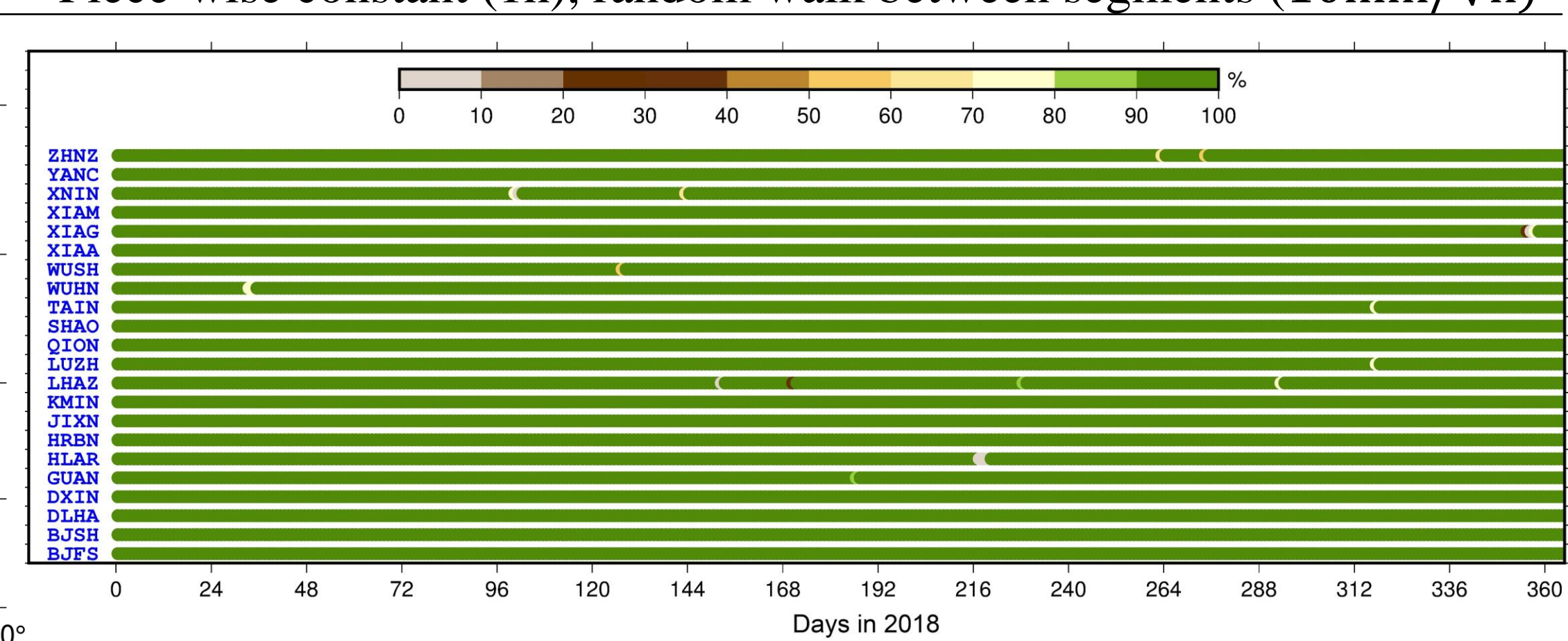


Fig. 2 The integrity of the ZTD products

### Results from typical station in each climate type region

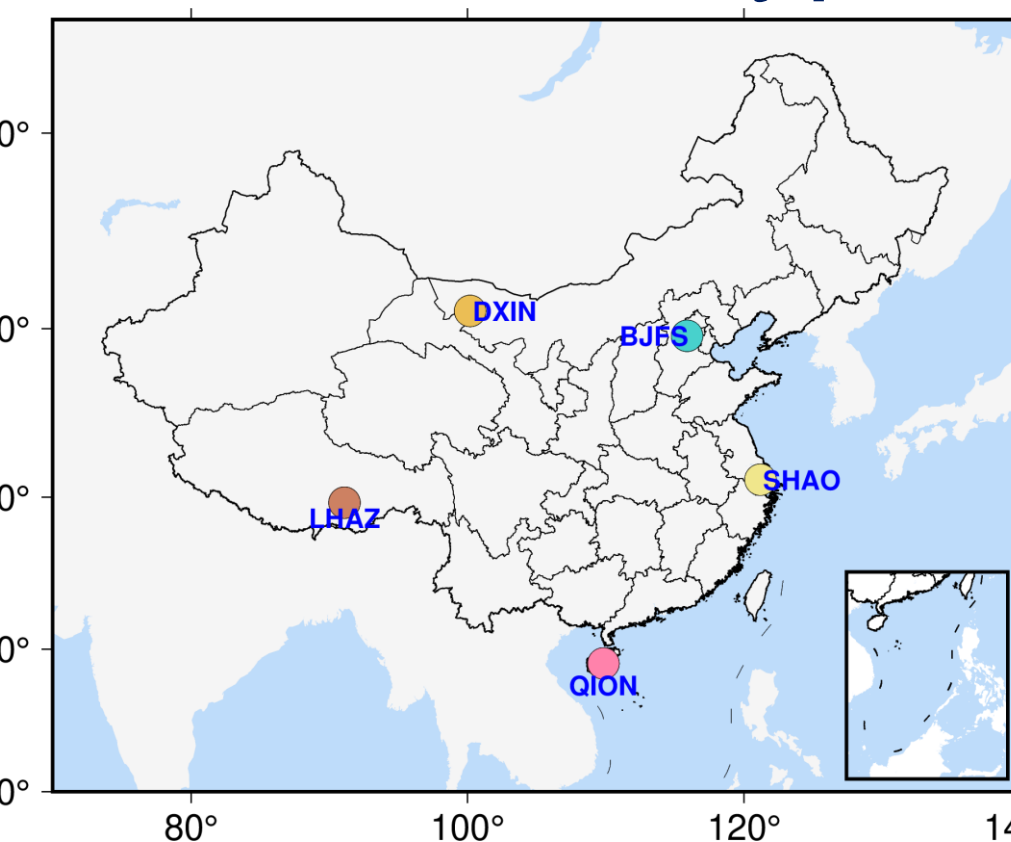


Fig.5 Geographical distribution of typical GPS stations

To analyze the SE signal variation characteristics of each climate type, we selected a station in each climate type region. We described and analyzed the variations of SE values from the five stations. And a statistical analysis of SWDs is presented in this section.

The time structure function defined as:

$$S(\tau) = \frac{1}{T} \int_{t=t_0}^{t=t_0+T} [SE(t, \theta_F, \lambda_F) - SE(t + \tau, \theta_F, \lambda_F)]^2 dt$$

The spatial covariance function limited to the hemisphere at a specific time epoch  $t_F$  was proposed as:

$$Cov(t_F, \Psi) = \int_{\alpha=0}^{\alpha=2\pi} \int_{\lambda=0}^{\lambda=2\pi} \int_{\theta=0}^{\theta=\pi/2} SE(t_F, \theta, \lambda) SE(t_F, \theta', \lambda') \cdot \cos(\theta) d\theta d\lambda d\alpha$$

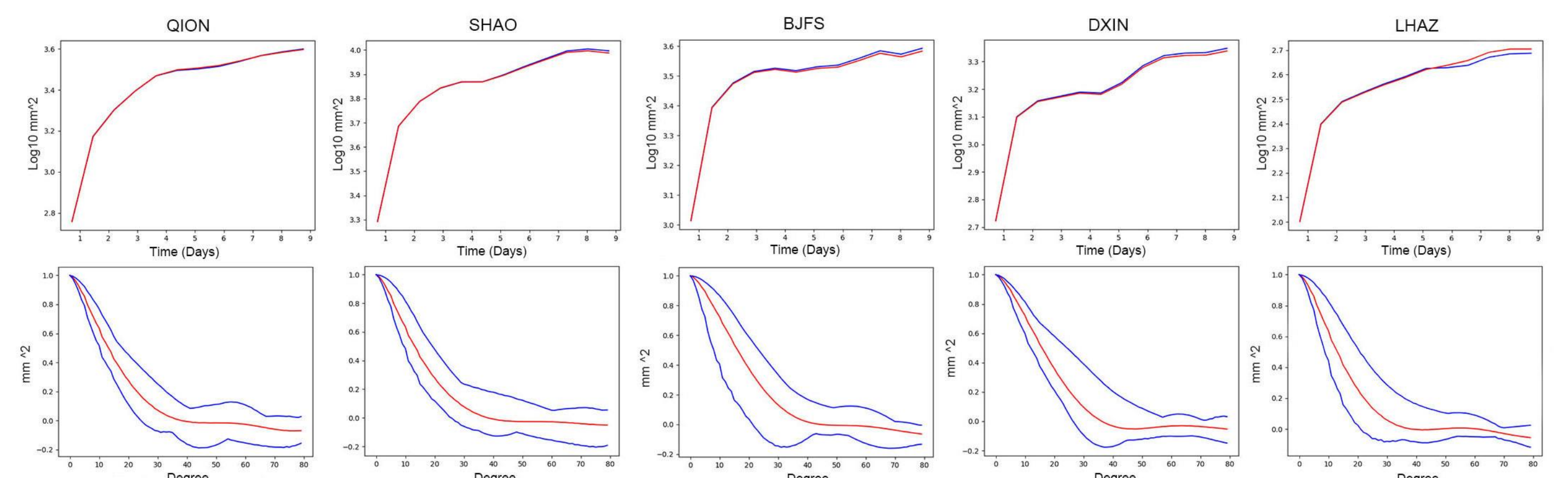


Fig.6 Log10 plot of the time structure function for GPS-derived SE signals over ten days (Top) and averaged spatial covariance function of GPS-derived SE signals over 2018 (Below)

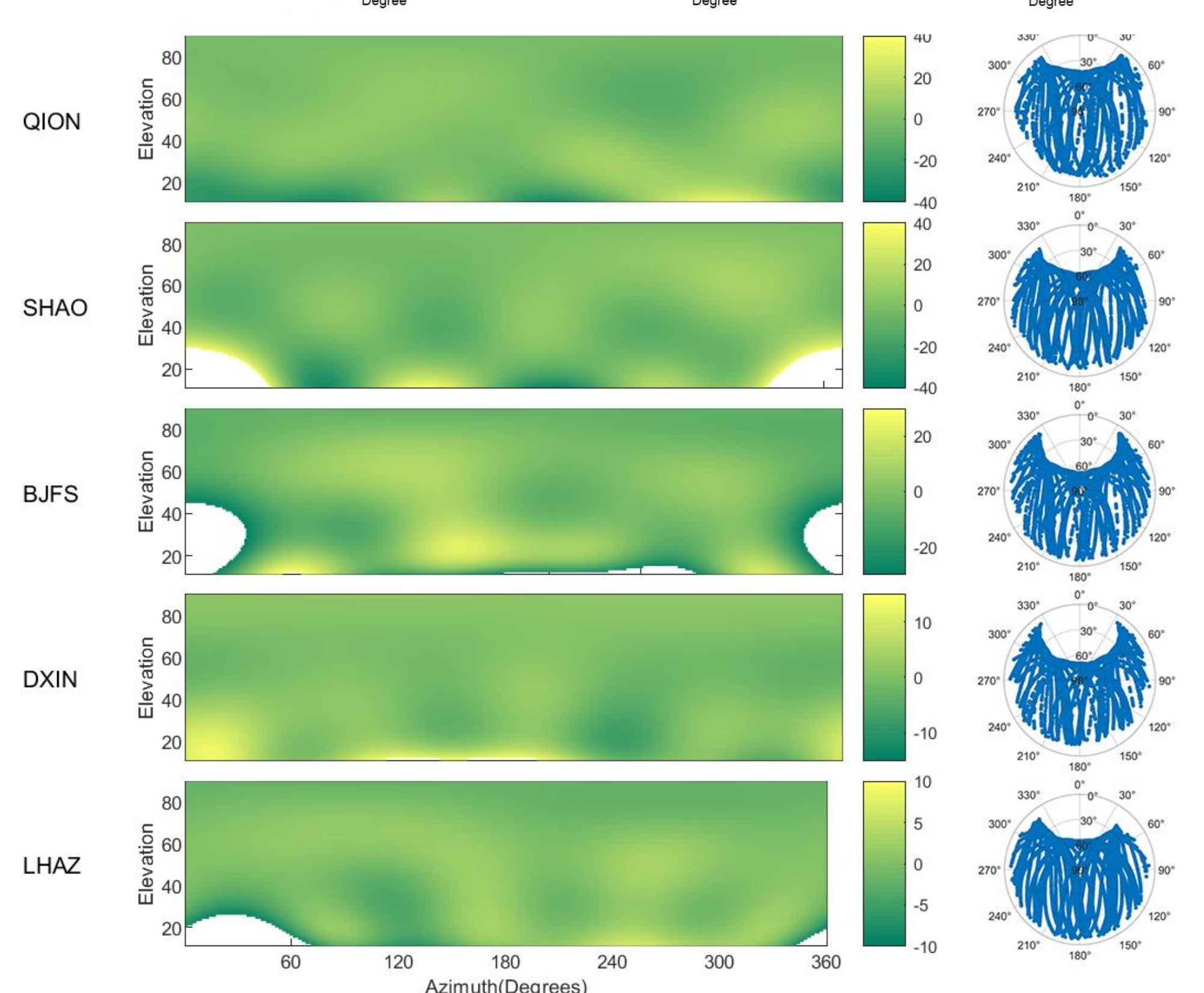


Fig. 7 Sky view of SE signals at the middle of September (left) in 2018 and sky tracks of the GPS satellites visible from the GPS stations in September 2018 (Colorbar: the variations of the SE values in mm)

#### Sub results

- ✓ The correlation length of SE signals at BJFS, QION, and SHAO stations is around four days.
- ✓ The spatial covariance lengths of SE signal at BJFS and DXIN are slightly higher than  $25^\circ$  (spherical distance). The lengths of LHAZ, SHAO and QION stations are almost slightly higher than  $20^\circ$ .
- ✓ SE signals show significant periodic variations within the azimuth range of  $0^\circ \sim 360^\circ$ , with a period of approximately  $120^\circ$ .
- ✓ The SE signals of QION and SHAO have the most obvious variations.